Electronic Supplementary Information

Glycerol oxidehydration to pyruvaldehyde over silver-based catalysts for improved lactic acid production

G. M. Lari,[a] R. García-Muelas,[b] C. Mondelli,[a]* N. López[b] and J. Pérez-Ramírez[a]*

[a] Institute for Chemical and Bioengineering, Department of Chemistry and Applied Biosciences, ETH Zürich, Vladimir-Prelog-Weg 1, CH-8093 Zürich, Switzerland. Tel: +41 44 6337120; E-mail addresses: cecilia.mondelli@chem.ethz.ch; jpr@chem.ethz.ch

[b] Institute of Chemical Research of Catalonia, ICIQ, The Barcelona Institute of Science and Technology, BIST, Av. Països Catalans 16, ES-43007 Tarragona, Spain.

Characterisation of the tin-containing zeolites

Powder X-ray diffraction (XRD) was performed using a PANalytical X'Pert PRO-MPD diffractometer with Ni-filtered Cu Kα radiation (λ = 0.1541 nm), acquiring data in the 5–70° 2θ range with a step size of 0.05° and a counting time of 8 s per step. The crystallinity was estimated from the ratio of the areas of the MFI reflections at 23.10°, 23.95° and 24.42° 2θ. UV-Vis spectroscopy was carried out in diffuse reflectance mode using an Ocean Optics Maya2000-Pro spectrometer. Prior to the analyses, samples were degassed at 313 K and 10^{-4} bar for 16 h. Spectra were collected in Kubelka-Munk units in the 200-600 nm range, with an integration time of 150 ms and accumulating 32 scans, and were corrected by subtracting the spectrum of the tin-free zeolite. Fourier transform infrared (FTIR) spectroscopy of adsorbed d_3-acetonitrile (Sigma-Aldrich, 99%) was conducted using a Bruker IFS66 spectrometer equipped with a liquid-N_2 cooled mercury cadmium telluride detector. Zeolite wafers (*ca*. 1 cm^2, 20 mg) were evacuated (10^{-3} mbar) for 4 h at 693 K prior to the adsorption of the probe molecule at room temperature. Spectra were recorded in the 650-4000 cm^{-1} range, with a resolution of 4 cm^{-1} and accumulating 32 scans.

Table S1. Initial conversion and selectivity data for supported metal catalysts in the conversion of GLY.[a]

Catalyst	X_{GLY} (%)	S_{Ac} (%)	S_{PAl} (%)	S_{PAc} (%)	S_{Acr} (%)	S_{AAc} (%)	S_{DHA} (%)	S_{GAl} (%)	S_{GAc} (%)	CB (%)
Al_2O_3-a	53	85	6	0	13	0	0	0	0	102
V/Al_2O_3-a	95	5	21	46	0	1	0	0	2	76
Ni/Al_2O_3-a	95	2	29	31	0	0	0	0	1	65
Fe/Al_2O_3-a	92	10	28	31	0	0	0	1	0	72
Sn/Al_2O_3-a	75	29	25	24	0	0	1	0	0	84
Cu/Al_2O_3-a	82	25	45	21	7	3	0	1	0	102
Ru/Al_2O_3-a	80	11	61	12	5	4	1	0	0	95
Ag/Al_2O_3-a	82	15	78	6	2	2	0	0	0	102
Pd/Al_2O_3-a	66	21	69	5	4	3	0	0	0	101
Pt/Al_2O_3-a	26	30	45	5	9	1	0	0	0	97
Au/Al_2O_3-a	13	39	75	4	2	0	0	0	0	103
Ag/Al_2O_3-b	52	12	75	4	1	0	0	0	0	96
Ag/Al_2O_3-c	15	15	81	3	1	1	0	0	0	100
Ag/Al_2O_3-d	21	18	71	5	0	0	0	0	0	99
Ag/SiO_2	0	30	80	5	0	0	0	0	0	100
Ag/ASA	81	12	21	31	51	25	0	0	0	132
Ag/Z940	6	7	51	9	0	0	0	0	0	98
Ag/Z40	64	21	14	7	51	21	0	0	0	109

[a] GLY: glycerol, Ac: acetol, PAl: pyruvaldehyde, PAc: pyruvic acid, Acr: acrolein, AAc: acrylic acid, DHA: dihydroxyacetone, GAl: glyceraldehyde, GAc: glyceric acid and CB: carbon balance. Reaction conditions: T = 623 K, P = 1 bar, C_{GLY} = 10 wt.%, $LHSV$ = 6 h^{-1}, O_2/GLY = 0.5 and t = 1 h.

Table S2. Characterisation data for the supports.

Support	S_{BET}[a] ($m^2\ g^{-1}$)	V_{pore}[b] ($cm^3\ g^{-1}$)	C_{Lewis}[c] (µmol g^{-1})	$C_{Brønsted}$[c] (µmol g^{-1})
Al_2O_3-a	85	0.50	81	4
Al_2O_3-b	68	0.39	48	2
Al_2O_3-c	73	0.51	24	1
Al_2O_3-d	69	0.61	17	2
SiO_2	130	0.40	0	1
ASA	78	0.45	6	56
Z940	317	0.19	1	2
Z40	511	0.25	82	177

[a] BET method; [b] Volume adsorbed at p/p_0 = 0.99; [c] FTIR spectroscopy of adsorbed pyridine.

Table S3. Calculated core-level shifts for the 3d transition of an Ag atom of a certain system with respect to an Ag atom in a bulk position in a clean metal slab. Vertex and side indicate the positions of Ag atoms in the 6-atom triangles identified on the AgO_x surface depicted in Figure 1b of the main manuscript. Experimental XPS data are reported in Figure 3c of the main manuscript.

System	Atom	Shift (eV)
Ag	surface	0.02
AgO_x/Ag	surface-vertex	0.68
	surface-side	0.48
	bulk	0.03
Ag_2O	surface	0.70
	bulk	0.86

Table S4. Initial conversion and selectivity data for supported silver catalysts in the conversion of Ac.[a]

Catalyst	X_{Ac} (%)	S_{PAl} (%)	S_{PAc} (%)	S_{Acr} (%)	S_{AAc} (%)	S_{DHA} (%)	S_{GAl} (%)	S_{GAc} (%)	CB (%)
Ag/Al_2O_3-a	81	95	4	0	0	0	0	0	96
Ag/SiC	76	95	5	0	0	0	0	0	94

[a] Ac: acetol, PAl: pyruvaldehyde, PAc: pyruvic acid, Acr: acrolein, AAc: acrylic acid, DHA: dihydroxyacetone, GAl: glyceraldehyde, GAc: glyceric acid and CB: carbon balance. Reaction conditions: T = 623 K, P = 1 bar, C_{Ac} = 8 wt.%, $LHSV$ = 6 h^{-1}, O_2/Ac = 0.5 and t = 1 h.

Table S5. Characterisation data for tin-containing zeolites.

Catalyst	Sn content[a] (wt. %)	S_{BET}[b] ($m^2\ g^{-1}$)	V_{pore}[c] ($cm^3\ g^{-1}$)	V_{micro}[d] ($cm^3\ g^{-1}$)	S_{meso}[d] ($m^2\ g^{-1}$)	Crystallinity[e] (%)
Z940	0.00	317	0.19	0.14	45	100
Sn-MFI	1.91	246	0.29	0.08	98	52
[Sn]BEA	1.52	527	0.29	0.20	16	-

[a] XRF spectroscopy; [b] BET method; [c] Volume adsorbed at p/p_0 = 0.99; [d] t-plot method; [e] XRD.

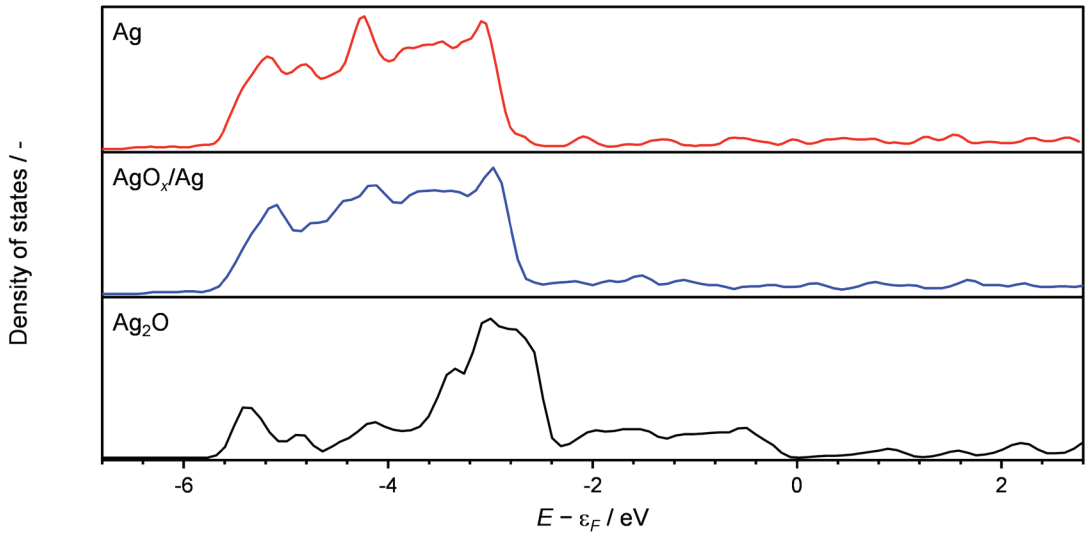

Figure S1. Density of states for Ag, AgO_x/Ag and Ag_2O surfaces. The energy values were referenced to the Fermi level (ε_F).

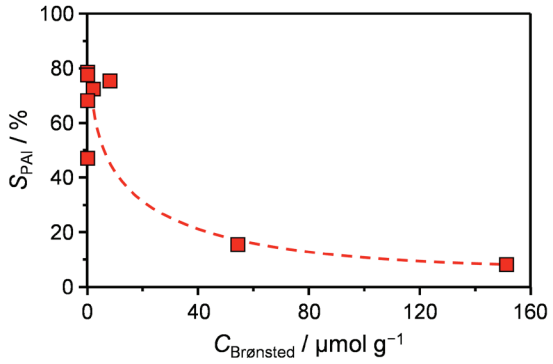

Figure S2. PAl selectivity as a function of the concentration of Brønsted-acid sites for Ag/Al_2O_3-a.

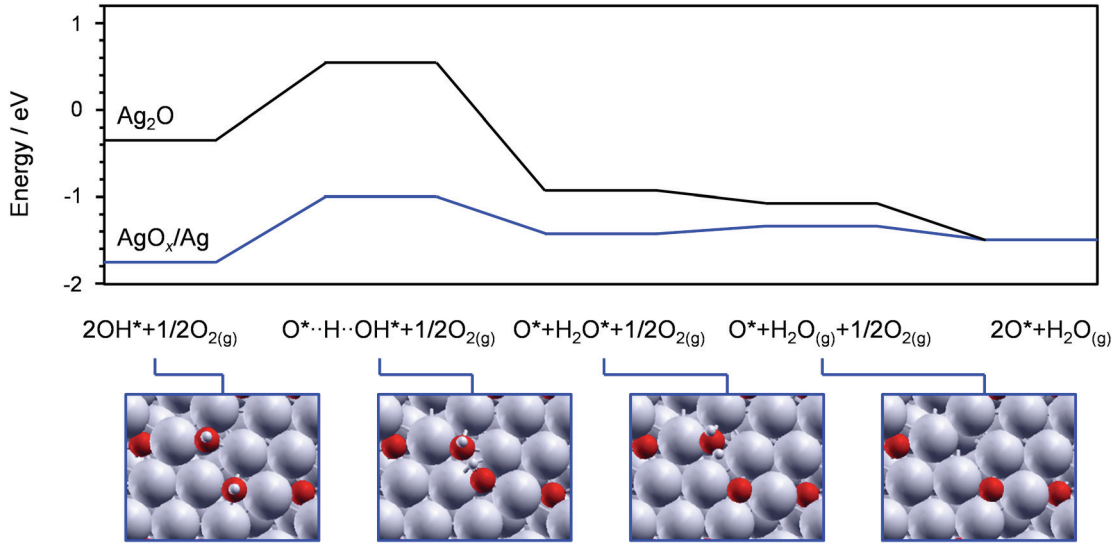

Figure S3. Energy profiles for the regeneration of the AgO_x/Ag and Ag_2O surfaces after the dehydrogenation of Ac and the corresponding structures calculated over the AgO_x/Ag surface.

The Ag models considered address the oxygen-lean (surface oxide) and oxygen-rich (bulk oxide) reaction regimes. The transition between the surface oxide and the bulk oxide, likely occurring at O_2/GLY ratios larger than 0.5, has not been characterised experimentally. However, insights into this scenario can be gathered placing an epitaxially-grown $Ag_2O(111)$ layer on Ag(111). The supercells of p(7×7) Ag(111) and p(3×3) Ag_2O (111) are commensurate, with a length of 20.88 Å. Therefore, a model consisting of two layers of Ag_2O supported on two layers of metallic silver was built (Figure S5). The simulation results, shown in Figure S6, demonstrate that $Ag_2O/Ag(111)$ qualitatively behaves similarly to pure Ag_2O. This indicates that the Ag_2O model would suffice to describe the catalyst at high O_2/GLY ratios.

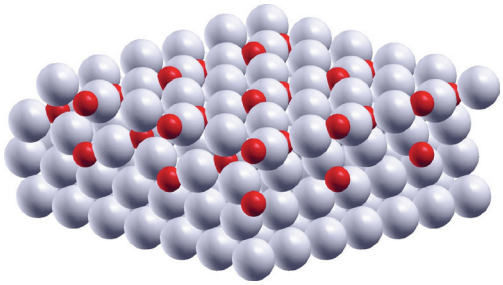

Figure S4. Representation of the Ag_2O/Ag surface.

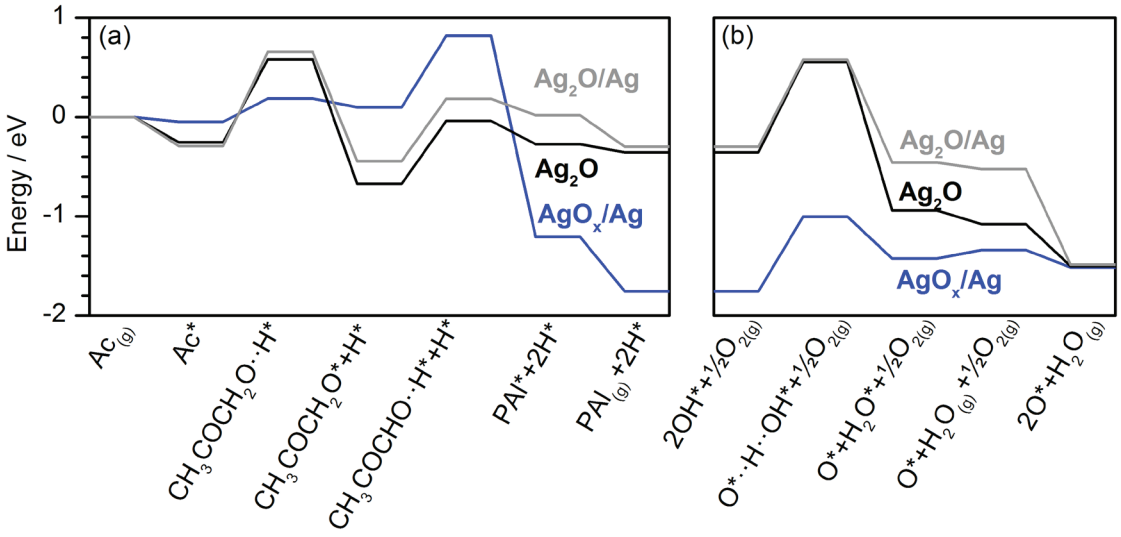

Figure S5. Energy profiles for (a) the dehydrogenation of Ac to PAl on AgO_x/Ag, Ag_2O and Ag_2O/Ag surfaces and (b) the regeneration of the catalysts.

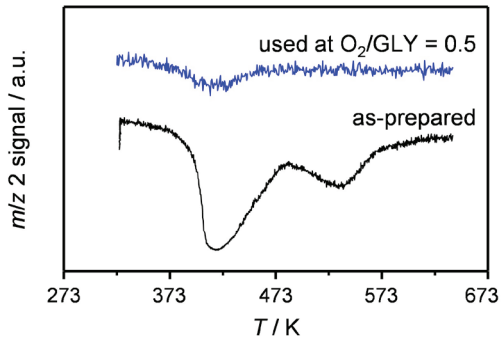

Figure S6. H_2-TPR characterisation of as-prepared and used Ag/Al_2O_3-d.

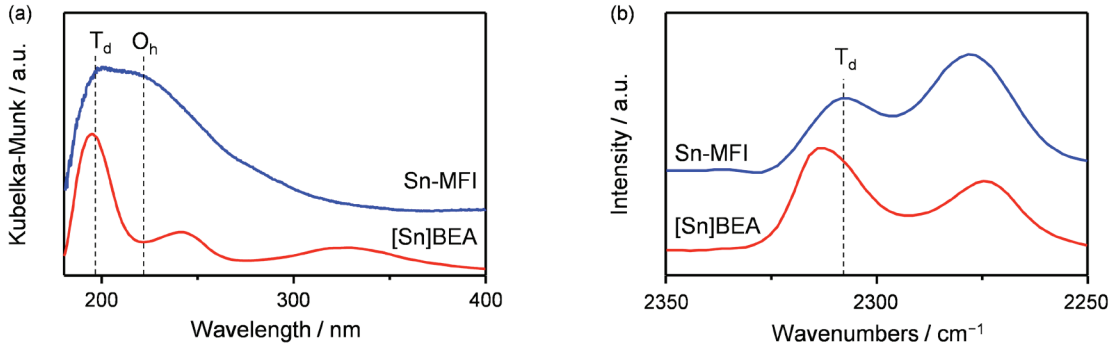

Figure S7. (a) UV-Vis spectra and (b) FTIR spectra of adsorbed d_3-acetonitrile for tin-containing zeolites.